Fe$_3$O$_4$-PDA-Lipase as Surface Functionalized Nano Biocatalyst for the Production of Biodiesel Using Waste Cooking Oil as Feedstock: Characterization and Process Optimization

Tooba Touqeer [1], Muhammad Waseem Mumtaz [1,*], Hamid Mukhtar [2], Ahmad Irfan [3,4], Sadia Akram [1], Aroosh Shabbir [2], Umer Rashid [5,*], Imededdine Arbi Nehdi [6,7] and Thomas Shean Yaw Choong [8]

[1] Department of Chemistry, University of Gujrat, Gujrat 50700, Pakistan; 17101707-035@uog.edu.pk (T.T.); sadia.nano@yahoo.com (S.A.)

[2] Institute of Industrial Biotechnology, Government College University, Lahore 54000, Pakistan; hamidwaseer@yahoo.com (H.M.); aroosh-gcu@hotmail.com (A.S.)

[3] Research Center for Advanced Materials Science, King Khalid University, Abha 61413, P.O. Box 9004, Saudi Arabia; irfaahmad@gmail.com

[4] Department of Chemistry, Faculty of Science, King Khalid University, Abha 61413, P.O. Box 9004, Saudi Arabia

[5] Institute of Advanced Technology, Universiti Putra Malaysia, Serdang 43400 UPM, Selangor, Malaysia

[6] Chemistry Department, College of Science, King Saud University, Riyadh 11451, Saudi Arabia; inahdi@ksu.edu.sa

[7] Laboratoire de Recherche LR18ES08, Chemistry Department, Science College, Tunis El Manar University, Tunis 2092, Tunisia

[8] Department of Chemical and Environmental Engineering, Universiti Putra Malaysia, Serdang 43400 UPM, Selangor, Malaysia; csthomas@upm.edu.my

* Correspondence: muhammad.waseem@uog.edu.pk (M.W.M.); umer.rashid@upm.edu.my (U.R.); Tel.: +60-3-9769-7393 (U.R.)

Abstract: Synthesis of surface modified/multi-functional nanoparticles has become a vital research area of material science. In the present work, iron oxide (Fe$_3$O$_4$) nanoparticles prepared by solvo-thermal method were functionalized by polydopamine. The catechol groups of polydopamine at the surface of nanoparticles provided the sites for the attachment of *Aspergillus terreus* AH-F2 lipase through adsorption, Schiff base and Michael addition mechanisms. The strategy was revealed to be facile and efficacious, as lipase immobilized on magnetic nanoparticles grant the edge of ease in recovery with utilizing external magnet and reusability of lipase. Maximum activity of free lipase was estimated to be 18.32 U/mg/min while activity of Fe$_3$O$_4$-PDA-Lipase was 17.82 U/mg/min (showing 97.27% residual activity). The lipase immobilized on polydopamine coated iron oxide (Fe$_3$O$_4$_PDA_Lipase) revealed better adoptability towards higher levels of temperature/pH comparative to free lipase. The synthesized (Fe$_3$O$_4$_PDA_Lipase) catalyst was employed for the preparation of biodiesel from waste cooking oil by enzymatic transesterification. Five factors response surface methodology was adopted for optimizing reaction conditions. The highest yield of biodiesel (92%) was achieved at 10% Fe$_3$O$_4$_PDA_Lipase percentage concentration, 6:1 CH$_3$OH to oil ratio, 37 °C temperature, 0.6% water content and 30 h of reaction time. The Fe$_3$O$_4$-PDA-Lipase activity was not very affected after first four cycles and retained 25.79% of its initial activity after seven cycles. The nanoparticles were characterized by FTIR (Fourier transfer infrared) Spectroscopy, XRD (X-ray diffraction) and TEM (transmission electron microscopy), grafting of polydopamine on nanoparticles was confirmed by FTIR and formation of biodiesel was evaluated by FTIR and GC-MS (gas chromatography-mass spectrometry) analysis.

1. Introduction

Overpopulation, urbanization, industrialization and augmentation of personal transport have increased the petroleum consumption immensely. It is predicted that petroleum reserves will become depleted soon if the rate of its consumption continue to increase with the same rate [1]. Depletion of non-renewable fuel reserves, elevation in price of fossil fuels and pollution caused by usage of petroleum products has spurred the production of eco-friendly, inexpensive alternative energy source that can reduce petroleum consumption and that is biodiesel [2]. Biodiesel has emerged as an alternative of petroleum due to its renewable nature, biodegradability, and interest of consumers in nature friendly products [3].

Feedstock selection for biodiesel production is of chief concern because of high prices associated with various feedstock. Edible and non-edible feedstocks have been used by many researchers for the biodiesel synthesis, edible oils including; sunflower, corn, rapeseed and soybean oil, while non edible oils including; Jatropha, *Eruca sativa*, Caster, Jojoba and other oils. Utilizing edible oils as feedstock will cause conflict with food production and food price so it is more desirable to use non edible oil [4]. A very economical feedstock is used cooking oil. Excess of waste frying/cooking oil is produced every day in restaurants and fast food shops. The use of edible oil for excessive frying/cooking at high temperature destroys the structure of triglyceride and produce the free fatty acids in oil, changing its pH, which is harmful for human health [5,6]. The oil is therefore being dumped off through drainage, which causes water pollution. This oil is useless and causes hazards to aquatic life. Using this waste oil to make something valuable is highly appreciated, because it is almost free feedstock for biodiesel production [7,8].

Transesterification is the preferred method for biodiesel production as compared to other techniques [9]. Various strategies of transesterification have been adopted to achieve better yield, purity and fast reaction rates. Catalytic transesterification is frequently used as, the presence of catalyst enhances the solubility of oil in alcohol and increases the reaction rate [10]. Catalysts of transesterification can be homogeneous or heterogeneous. Homogenous catalysts include; acid and alkaline catalyst. Alkaline catalysts are commonly used because of their low cost and higher catalytic activity at ambient conditions, while alkaline catalysts do not work efficiently under higher FFA conditions [11]. Besides that, there are many drawbacks of using these catalysts in excess which includes; formation of toxic waste that need to be neutralized by several washings, hence it causes environmental pollution, contaminated glycerol is produced, purification of this glycerol increases the production cost, partial saponification can lead to the production of soap which makes it difficult to separate glycerol and alkyl esters hence decreases the yield of biodiesel [12]. Furthermore, another major drawback is that these catalysts cannot be reused or recycled.

Heterogenous catalysts include; enzymes (lipase), alkaline earth metals, zirconias of potassium and silicates of titanium etc. The enzyme used for transesterification is usually lipase. Lipase has several advantages over convention alkali catalysts; e.g., there is no need of purification of biodiesel after transesterification thus no toxic waste is produced—especially in case of waste cooking oil, where there are lot of free fatty acids, lipase reduces the chance of saponification [13]. However, there are some reasons that hampered its utilization, which include; high cost, difficulty in its recovery and instability at high temperature and pH. The best strategy to tackle these problems is the immobilization of enzyme on some support. Previously, lipases have been immobilized on several surfaces such as; ceramics, calcium alginate beads and other inorganic matrixes, which increase the thermal stability of the enzyme. However, the activity of the enzyme is revealed to be reduced due to a decrease in conformational flexibility and capability of adsorption on support surface [14]. Another effective way

of using bio-catalyst is to immobilize it on nano-support. Different techniques such as; entrapment, adsorption and covalent immobilization are being used for this purpose. Enzymes immobilized on nanoparticles provide the advantage of greater enzymatic activity, better selectivity along with thermal stability, adaptability towards wider pH range, easy recovery and purification [15]. If the nanoparticles used for immobilization are metal oxides, then these particles provide the advantage of low pricing, and higher stability even in harsh conditions, another advantageous attribute of metal oxide nanoparticles (NPs) is their magnetic property. Nanoparticles of iron, nickel, cobalt, chromium, manganese and their oxides show enhanced magnetic moment as compared to other metals [16]. Among these metal oxides, iron oxides—especially magnetite Fe_3O_4—shows very strong magnetism and it is also less toxic when compared to nickel and cobalt. Enzyme was first immobilized on magnetic nanoparticles surface by Matsunaga and Kamiya [17]. Immobilizing lipase on magnetite will generate a nano-biocatalyst, which will grant the edge of better activity in harsh conditions and reusability [18].

To reduce the risk of toxicity and make them more biocompatible, the surface of nanoparticles can be modified with different polymers using "graft to and graft from methods". Polymers (natural/synthetic) are used as coatings that also provide active groups at the surface to afford immobilization of lipase on nanoparticles. These polymers mostly contain epoxy and amine groups that react with active groups of lipases. However, the drawback of using polymers with amine group is the need of activation of amine group using some aldehydes, most commonly, amine group activation is done using gutaraldehyde [19]. This activation step increases the cost and preparation time of catalyst.

A versatile coating for the nanoparticles is polydopamine (formed by self-polymerization of dopamine monomers through oxidation in slightly alkaline conditions). Dopamine contains catechol as well as amine group, which efficiently interacts with metal oxide nanoparticles [20]. In an alkaline medium on oxidation, the catechol group of dopamine converts to the indo-5, 6-quinone, which further undergoes series of inter/intra molecular reactions, forming polydopamine grafted on the NPs surface. The residual quinone and catechol groups present on the surface after polymerization are reactive towards nucleophiles such as thiol and amine groups. These groups of lipases covalently immobilize the lipase on polydopamine through Schiff base formation and Michael addition reaction. Lipase immobilized on polydopamine containing nanoparticles show higher efficiency and higher enzyme loading as compared to the immobilization at naked nanoparticles [21]. The present work was therefore planned to prepare magnetic metal oxide nanoparticles by solvothermal method followed by polydopamine grafting and immobilization of *Aspergillus terrus* lipase for development of nano-biocatalyst. The synthesized nano-biocatalyst was then employed for the synthesis of biodiesel.

2. Materials and Methods

All the chemicals/reagents used, i.e., $FeCl_3 \cdot 6H_2O$, ethylene glycol, ethylene diamine, sodium acetate, methanol, ethanol, potassium iodide, iodine, n-hexane, chloroform, toluene, acetic acid, distilled water, potassium hydroxide, hydrochloric acid, phenolphthalein and isopropanol etc., were of analytical research grade obtained from Sigma-Aldrich (St. Louis, MO, USA). Lipase was produced from *Aspergillus terreus* AH-F2. The feedstock waste cooking oil was obtained from local restaurant situated in district Gujrat Pakistan.

2.1. Preparation of Nanoparticles

Fe_3O_4 nanoparticles were prepared/synthesized by solvothermal method by Guoet al. [22] with some modifications. One gram of $FeCl_3 \cdot 6H_2O$ was added in 20 mL of ethylene glycol and stirred to get a clear solution, then 3 g of sodium acetate and 10 mL of ethylene diamine were added in the solution, which was stirred for 30 min at room temperature. The mixture was then enclosed in a 50 mL Teflon lined autoclave and it was heated in oven for 8 h at 180 °C. The black colour product obtained was washed with successive distilled water/ethanol rinses followed by product drying using a desiccator. Black magnetic powder was obtained after drying.

2.2. Grafting of Dopamine on Fe₃O₄ Nanoparticles

Dopamine was coated on nanoparticles using "graft from" technique [23]. 0.1 g of Fe_3O_4 nanoparticles were suspended in 20 mL of distilled water. Afterwards, 20 mL of 20 milli molar tris-HCl buffer having pH 8.5 was introduced in the suspension. Then, 0.1 g of dopamine hydrochloride was slowly added in the suspension (2 mg/15 s) and the suspension was stirred for 1 h. Nanoparticles coated with polydopamine were formed by the self-polymerization of dopamine in alkaline conditions.

2.3. Characterization of Nanoparticles and PDA-Nanoparticles Complex

(a) Nanoparticles were characterized by X-ray diffraction, which helps to identify the crystal phase, dimensions and size of the crystalline material. X'pertpro (PANalyatical) XRD model was used for this purpose. The XRD pattern of Fe_3O_4 was attained by use of Cu K alpha radiation of wave length 1.54 Å. The patron was taken between the range 20–80 θ with 0.02 scan step size.

(b) Morphological characterization was carried out by TEM (Tecnai G^2 F20 U-TWIN) with an accelerating voltage of 200 kV.

(c) Bare nanoparticles and the nanoparticles after grafting of polydopamine were analysed by FTIR in the scanning range 400–4000 cm^{-1}, using the Cary 630 Agilent FTIR spectrometer to check the formation/purity of nanoparticles and to confirm the attachment of dopamine polymers on nanoparticle surface.

2.4. Lipase Immobilization on Modified Nanoparticles

Lipase was produced from *Aspergillus terreus* AH-F2 and purified using the method described in previous work of our research group [24]. Into 40 mL of phosphate buffer with pH 7, 0.40 g of lipase was added. The suspension of polydopamine coated magnetic nanoparticles was added slowly to the mixture of lipase with vigorous stirring for 3 h at 4 °C. The nucleophilic groups present in lipase such as thiol and amines reacted with the residual catechole and quinone groups present at the surface of Fe_3O_4-PDA nanoparticles by Schiff base and Michael addition mechanisms and were immobilized without the need of any coupling and activating agents (Figure 1). The protein content before and after the immobilization process was determined to check the immobilization yield using Bradford's method. The formed nano-biocatalyst was washed several times with phosphate buffer to remove any unreacted lipase and then freeze dried [23,25].
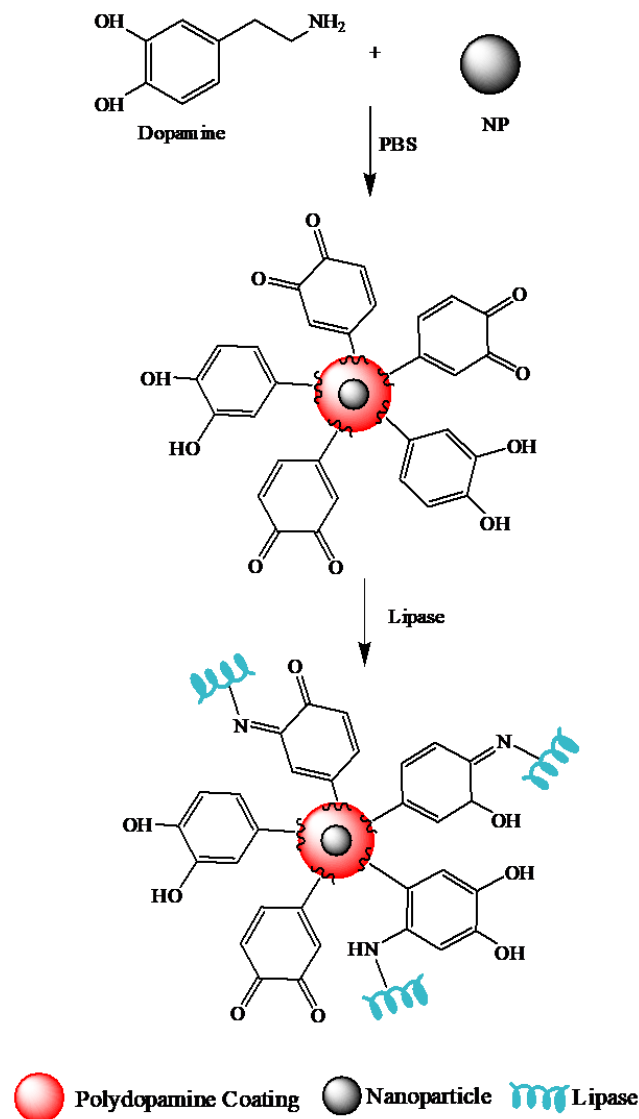
Figure 1. Schematic representation of lipase immobilization on dopamine coated.

2.5. Lipase Activity Assay (Free and Immobilized Form)

Lipase assay for free and immobilized lipase was performed by using the titrimetric method [24]. The activity of lipase was measured by the titration of fatty acids, which were produced from oil while reacting with enzyme. The assay reaction mixture (consisted of 1 mL of free lipase (produced from *Aspergillus terreus* AH-F2) while 0.1 g of nano-biocatalyst in the case of immobilized lipase and 10 mL of olive oil (10%)) was homogenized in 10 g of gum acacia and phosphate buffer (5 mL) with pH 7 followed by the addition of 0.6% calcium chloride (2 mL). This mixture was then incubated for 1 h in a water bath shaker at 37 °C. After incubation, the enzymatic reaction was ceased by adding 20 mL of ethanol/acetone mixture (1:1) following the addition of few phenolphthalein drops. The quantity of fatty acids released during this period by the action of lipase was titrated by using 0.1 N NaOH solution.

One unit of lipase activity (U) was defined as the amount of enzyme which released one micro mole (μmol) of fatty acid per minute under specified assay conditions.

Lipase units were determinedLipase units were determined as follows:

$$\text{Lipase Activity (U/mg/min)} = \frac{\Delta V \times N}{m(\text{sample})} \times \frac{1000}{60}$$

where $\Delta V = V2 - V1$; V1 = volume of NaOH consumed against control flask; V2 = volume of NaOH consumed against experimental flask; N = normality of NaOH; m(sample) = mass of enzyme extract; 60 = time of incubation (min) for bacterial lipase.

The effects of pH and temperature on the activity of free and immobilized lipase were studied using the above-mentioned assay method. The impact of pH on catalytic activity was investigated by incubating the sample at 37 °C with the phosphate buffer within pH range 5 to 10, whereas the impact of temperature in the range 25–50 °C was also studied at optimum pH levels.

2.6. Collection and Characterization of Feedstock

WCO (waste cooking oil) was collected from the local restaurant for the biodiesel production. The feedstock was purified by filtration to remove any food chunks and inorganic material in the waste oil. The physico-chemical properties of WCO biodiesel were analysed to reveal the quality of the used oil. Iodine number, specific gravity, density, peroxide value, acid value, saponification value and refractive index of the oil were calculated using standard analytical AOCS (American oil chemist's society) methods.

2.7. Experimental Design

Process of biodiesel production using Fe_3O_4_PDA_Lipase was optimized using five factor CCRSM (central composite response surface methodology) provided by Design Expert version 10.0.7 (State-Ease Inc., Minneapolis, MN, USA). The five independent variables chosen for the investigation of the optimization process with their ranges are A (methanol/oil ratio 3:1 to 9:1), B (biocatalyst concentration 1 to 10%), C (reaction temperature 20 to 50 °C), D (reaction time 12 to 48 h) and E (water content 0.2 to 1%). Fifty reactions were carried out as per experimental design.

A reaction mixture containing a specified amount of oil, nano-biocatalyst, methanol and water were allowed to react in a conical flask placed in shaking incubator, while reaction parameters were set in accordance to the RSM (response surface methodology) design. After completion of reaction, the glycerol was separated from biodiesel. Crude biodiesel was purified, and remaining methanol was recovered by using a rotary evaporator under the conditions of reduced pressure. GC-FID, having a highly-polar BPX-70 capillary column (30 m × 0.25 mm), was utilized for the analysis of products. The oven temperature was kept at 100 °C for 30 s, then raised to 250 °C at a rate of 10 °C/min, while the temperature of the detector was set at 270 °C. 500 ppm of sample was dissolved in hexane containing methyl heptadecanoate as an internal standard, and 1 μL of this mixture was injected in column [26,27]. The percentage conversion of biodiesel was calculated by given formula [28]

$$\text{FAME (Biodiesel) \%} = \frac{\sum A_{ME} - A_{IS}}{A_{IS}} \times \frac{C_{IS} \times V}{M} \times 100$$

where $\sum A_{ME}$ denotes the sum of peak areas of FAME's peaks, A_{IS} is the peak area of the internal standard peak (methyl heptadecanoate), C_{IS} is the concentration of the internal standard, V is the volume of the internal standard and M is the mass of biodiesel.

2.8. Recovery and Recycling of Nano-Biocatalyst

The Fe_3O_4_PDA_Lipase was recovered by magnetic decantation from both the biodiesel and glycerol layers. Separated Fe_3O_4_PDA_Lipase was then washed and dried at ambient temperature for reuse.

2.9. Characterization of Biodiesel

Biodiesel produced by Fe_3O_4_PDA_Lipase catalyzed transesterification was monitored by Fourier transfer infrared (FTIR) spectroscopy. The FTIR spectra of feedstock and synthesized biodiesel were taken over the scanning range 400–4000 cm^{-1} using Cary 630 Agilent FTIR spectrometer. Oil FTIR

spectra was compared to the FTIR of synthesized biodiesel to confirm the formation of fatty acid methyl esters. The GC/MS scan of biodiesel was taken to reveal compositional profile of synthesized biodiesel. GCMS QP 2010 system with a dB 5 column and a diameter of 0.15 mm was used. One μL sample size and 1:100 split ratio was selected. Helium as the carrier gas at 1.2 mL/min rate was used to elute the sample. The column temperature was set in the range 150–250 °C, at rate of 4 °C/min. GCMS mass scanning range was 30 to 550 m/z. Detection of FAMEs was done using NIST MS library of GCMS. The compatibility of WCO based biodiesel being used as fuel was confirmed by the estimation of its fuel properties, which were investigated according to the ASTM D methods.

2.10. Selection of Suitable Models for Optimization

Based on the experimental outputs, the best fitted model out of linear, 2Fi, cubical and quadratic models were selected for optimization purpose. The fitness of selected models was further ascertained through summery statistics such as R^2, adjusted R^2, model significance and lack-of-fit test. Moreover, normality and predicted values versus actual values plots were also employed for the above said purpose. The impact of selected reaction variables on the response i.e., biodiesel yield was revealed by 3D response surface plots.

3. Results and Discussion

3.1. Synthesis and Evaluation of Nano-Biocatalyst Effectiveness

3.1.1. XRD Analysis

The XRD pattern of Fe_3O_4 nanoparticles formed by solvothermal method is shown in Figure 2. The XRD pattern of formed nanoparticles resembles with JCPDS card No# 019–0629 for magnetite, with no extraneous peak, which indicates the high purity of the magnetite. The 2-theta value of peaks were 29.95°, 35.05°, 42.73°, 53.37°, 56.63°, and 62.29°, which attribute to the interplanar spacing or d value in angstrom with their (hkl) of 2.98 (220), 2.56 (311), 2.12 (400), 1.72 (422), 1.62 (511) and 1.49 (440), respectively. The peak values resemble with characteristic XRD peaks of Fe_3O_4 lattice with cubic spinal shape. The sharp peaks correspond to the high crystallinity of the magnetite. The particle size calculated using Scherrer equation was 24.18 nm, which is close to the value calculated by TEM images showing homogeneity in the particle sizes. The result has resembled with previously reported results [29,30].
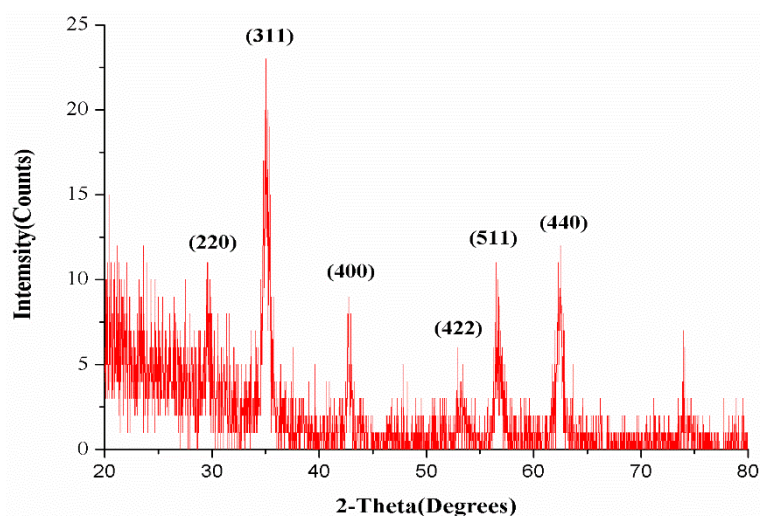

Figure 2. XRD (X-ray diffraction) graph of Fe_3O_4 nanoparticles.

3.1.2. TEM Analysis

TEM analysis was done for a detailed investigation of morphological characters. TEM images of the magnetic nanoparticles (Figure 3) were used to confirm the size and the shape of the nanoparticles. One can see from Figure 3a,b, that all the nanoparticles are homogeneous in size and shape. The size calculated using the TEM images ranges from 24 to 27 nm, whereas the shape is almost round. No agglomeration appeared in the micrograph, which may attribute to the homogeneous depression of these nanoparticles. TEM image (Figure 3c) shows that the nanoparticles have a mesoporous structure, which helps to achieve better catalytic properties.
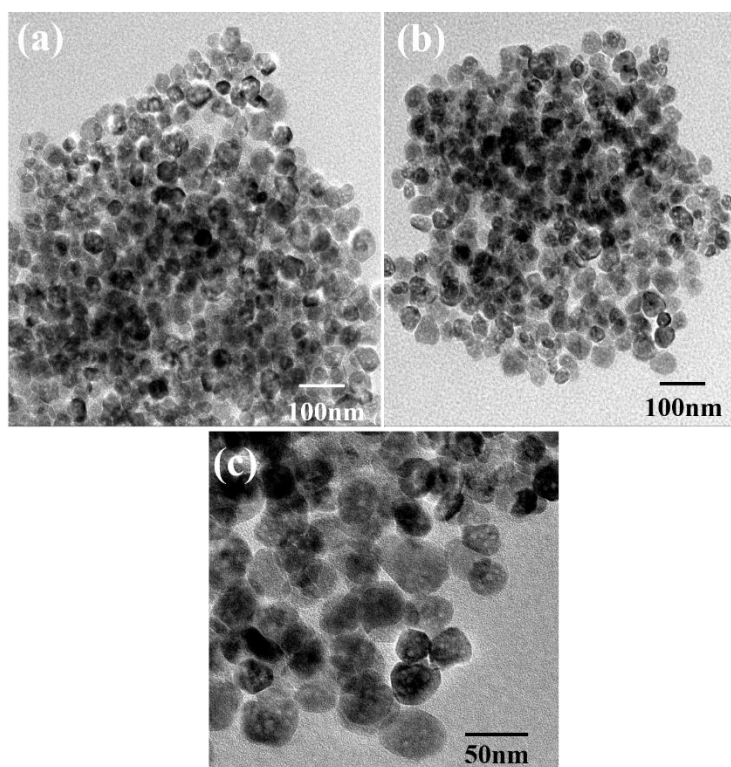

Figure 3. TEM images of the Fe_3O_4 nanoparticles at (**a**) 100 nm; (**b**) 100 nm and (**c**) 50 nm magnifications.

3.1.3. FTIR Analysis of Nanoparticles

A small amount of the product formed by the addition of dopamine in Fe_3O_4 suspension was taken out, washed with distilled water and dried using desiccator. The dried product was then subjected to Fourier transfer infrared spectroscopic analysis. FTIR confirms the attachment of dopamine on iron oxide nanoparticles by the presence of four peaks. Absorption band at 3209 cm^{-1} corresponds to the characteristic starching frequency of hydroxyl groups merged with a starching frequency band of N-H. This broad band was due to catechol groups of dopamine at the surface. Bending vibration peak of N-H was at 1628 cm^{-1}. Sharp peak at 1290 cm^{-1} indicated the presence of C-O bond. While peak at 1472 cm^{-1} was attributed to the C=C ring starching band overlapped with –CH_2 scissoring band (Figure 4). The results were depicted to be comparable to previous research [24].
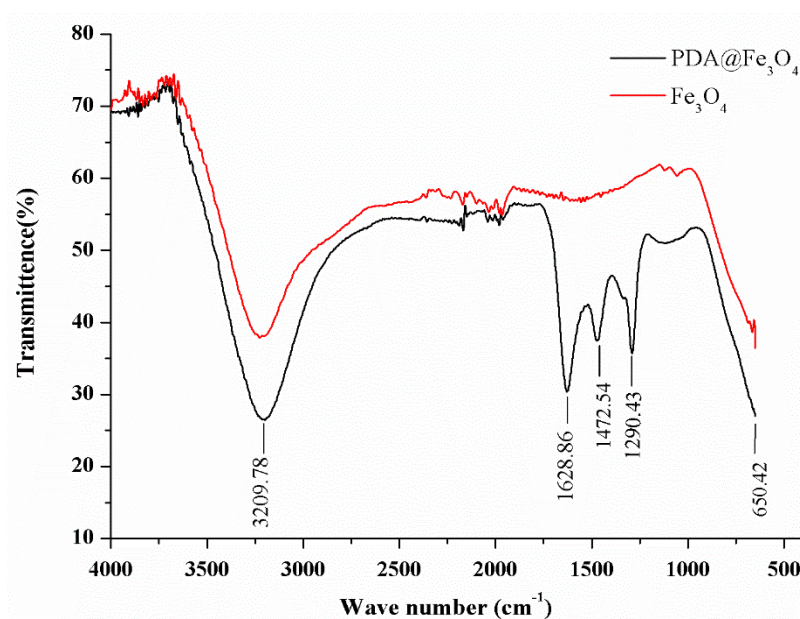
Figure 4. Comparative FTIR of naked Fe_3O_4 and polydopamine coated Fe_3O_4 nanoparticles.

3.1.4. Lipase Activity Assay

The activity titer of free lipase was found to be 18.32 U/mg/min, while the activity titer of $Fe_3O_4\_PDA\_Lipase$ was found to be 17.83 U/mg/min. Lipase loading of 0.336 g (84.2% of used enzyme) was achieved by using polydopamine functionalized Fe_3O_4. The results showed that polydopamine gave high lipase loading and lipase activity because the complex formed by the combination of polydopamine and Fe_3O_4 nanoparticles was found to be efficient regarding the immobilization of lipase providing wider surface during the reactions, hence gave higher conversion rate in a short period of time [31].

3.1.5. Effect of pH on Nano-Biocatalyst Activity

The impact of pH on the activities of free and immobilized lipase was studied to find the optimum pH of enzyme activity. The effect of pH in the range of 5 to 10 was studied (Figure 5), and it was found that maximum lipase activity was exhibited at pH 7.0 for free lipase (i.e., 18.32 U/mg/min taken as 100% for free lipase) while lipase immobilized on Fe_3O_4 nanoparticles gave maximum activity at pH 8 (i.e., 17.83 U/mg/min taken as 100% for immobilized lipase). Above and below this pH, lipase activity was reduced. The results showed that, the relationship curve between pH and activity of lipase immobilized on Fe_3O_4 nanoparticles was shifted towards the right, which demonstrate that due to lipase immobilization on functionalized magnetic nanoparticles, the ability of lipase tolerance increased even if the pH of the reaction mixture varied. This means that by the immobilization of lipase, its adaptability to a wide pH range increased as compared to free lipase. Our studies were in accordance with the studies of Baharfar and Mahajer, in which magnetic nanoparticles were used for the immobilization of lipase, and immobilized lipase gave maximum activity at increased pH as compared to free lipase [31].
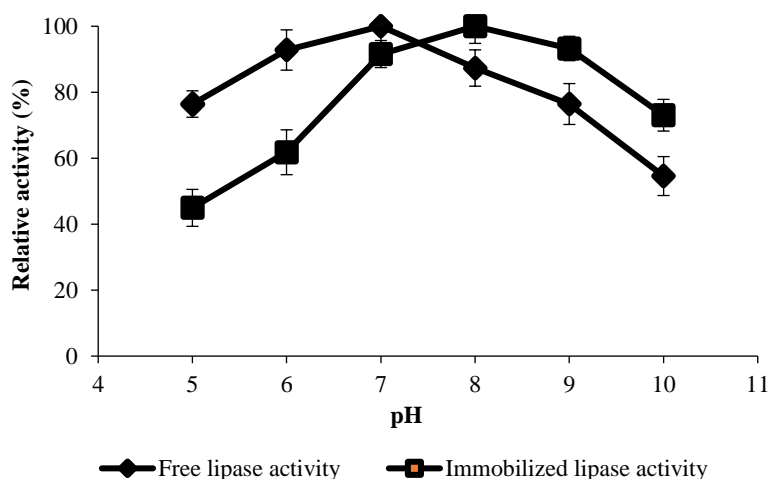
Figure 5. Effect of pH on the activities of free and immobilized lipase (date points are the mean of triplicate reaction values).

3.1.6. Effect of Temperature on Activity of Nano-Biocatalyst

The impact of temperature on the activity of free and immobilized lipase was studied in the range of 25 to 50 °C (Figure 6) and it was depicted that maximum activity of free lipase was obtained at 37 °C, while the lipase immobilized on Fe_3O_4 nanoparticles showed maximum activity at the temperature of 40 °C, which means that lipase immobilized on nanoparticles was tolerant to high temperature fluctuations and was stable at a wider temperature range. The covalent bonds formed during immobilization may have increased the stability and tolerability of the lipase. Similar studies were reported by other researchers [23,31].
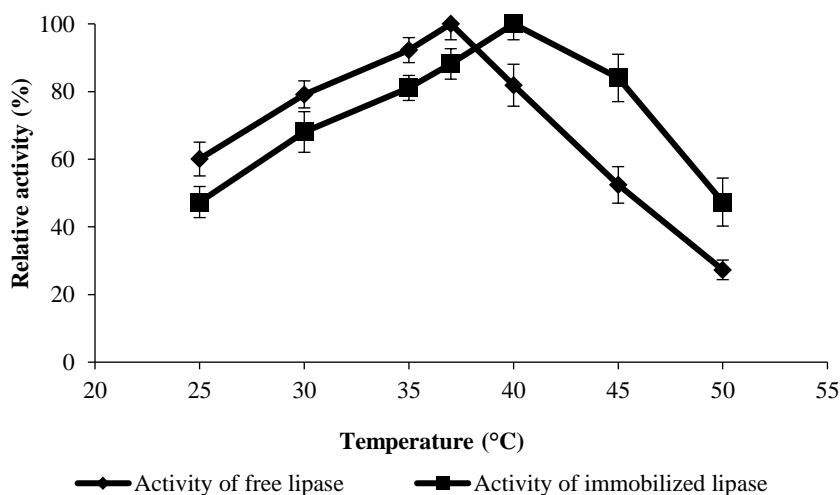

Figure 6. Effect of temperature on the activities of free and immobilized lipase (date points are the mean of triplicate reaction values).

3.2. Process Optimization/Characterization

3.2.1. Characteristics of Feedstock

The density and the specific gravity of feedstock were 0.918 ± 0.050 g/cm^3 and 0.934 ± 0.051 respectively, while the acid value was calculated to be 1.68 ± 0.12 mg/KOHg, the peroxide value was 15.80 ± 0.32 mEq/Kg, iodine value was 96.20 ± 1.00 and the saponification value of waste cooking oil feedstock was 182.0 ± 1.0 mg KOH/g.

3.2.2. Composition Analysis of Produced Biodiesel by GC-MS

The product (biodiesel) was analysed by GC-MS. Major fatty acid methyl esters consisted of methyl esters of palmitic acid (16:0), lenoleic acid (18:2), stearic acid (18:0), gonodic acid (20:1) and arachidic acid (20:0) were identified by NIST library of GC-MS. Noshadi et al. [32] reported waste cooking oil with myristic acid, palmitoleic acid, palmitic acid, stearic acid, oleic acid, linoleic acid and linolenic acid. Uzun et al. [33] used waste oils for biodiesel production with a following fatty acid content of palmitic acid, stearic acid, oleic acid, linoleic acid and docasanoic acid. Comparable results have also been reported by [34–36], who found that the variations in fatty acid content might be due to presence of different edible oils and their varying amounts in cooking oils.

3.2.3. FTIR Monitoring of Biodiesel Production

Conversion of triglycerides into the biodiesel was confirmed by the FTIR spectral comparison of feedstock oil with the synthesized biodiesel. Characteristic peaks of waste cooking oil were observed at 723, 1700–1800 and 2800–3000 cm^{-1}, which corresponds to –CH$_2$ rocking, C=O starching and symmetric C-H stretching vibrations, respectively. While in the case of biodiesel, adsorption peak at 1437 cm^{-1} corresponding to methyl ester and peak appearing at 1196 cm^{-1} for C-O ester bond are the characteristic biodiesel adsorption peaks. The absence of 1380 cm^{-1} peak in biodiesel that represents the O–CH$_2$ bonds in glycerol site of triglycerides further proves the formation of methyl esters (Figure 7). The results obtained in the present work are comparable to previous research [37–39].
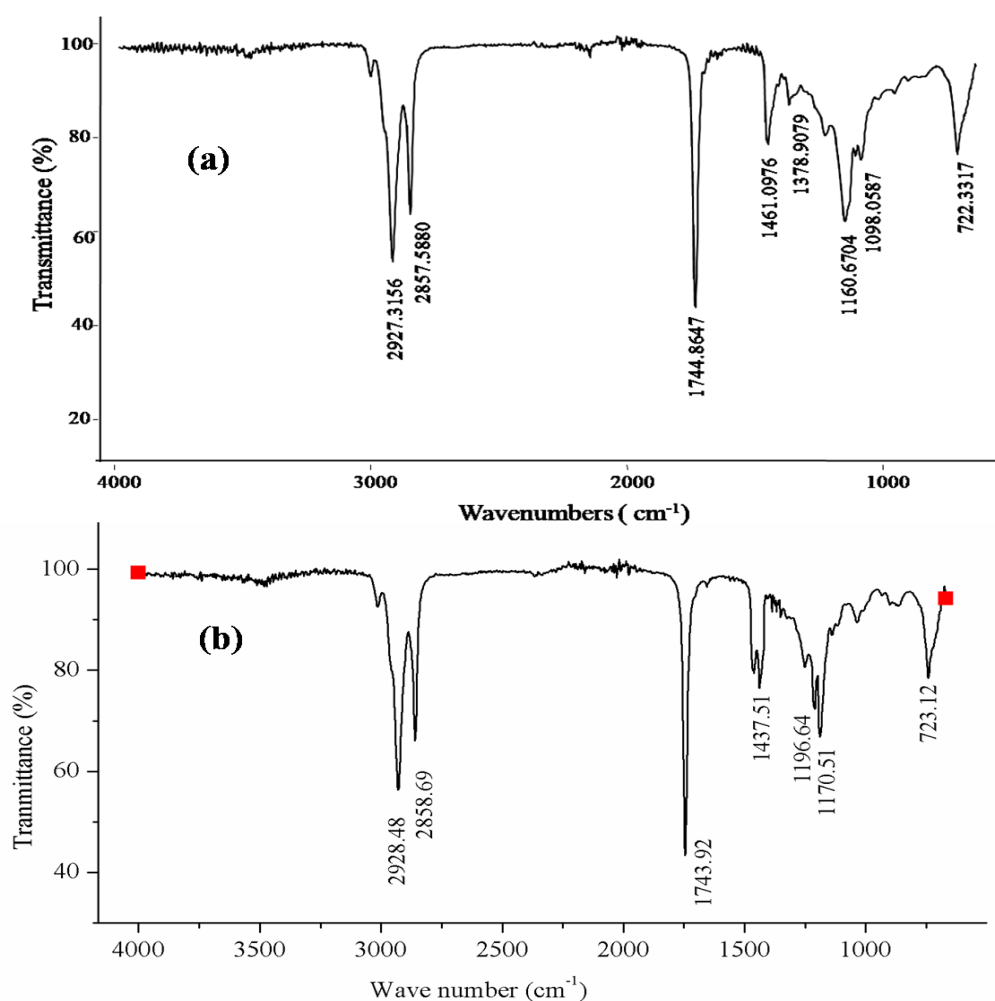

Figure 7. FTIR of (**a**) WCO and (**b**) WCO based biodiesel.

3.2.4. Optimized Reaction Parameters

Table 1 describes the optimum reaction conditions for the optimized yield of waste cooking oil-based biodiesel. By carrying out 50 experiments on various conditions of selected parameters, it has been observed that Fe_3O_4_PDA_Lipase catalysed the transesterification of feedstock oil giving a maximum yield of 92%, under the given set of reaction conditions/parameters viz., biocatalyst concentration (10%), CH_3OH to oil molar ratio (6:1), reaction time (30 h), reaction temperature (37 °C) and water content (0.6%). While biocatalyst concentration (1%), methanol to oil molar ratio (3:1), reaction time (12 h), reaction temperature (20 °C) and water content (1%) gave the lowest response (41.5%).

Stoichiometrically, methanol reacts with triglycerides in 3:1 molar ratio, but excess amount of methanol was provided to increase the rate of forward reaction because transesterification is equilibrium limited reaction [40]. Moreover, the viscosity of the oils is high, which hinders the mass transfer. The addition of excess methanol lessens the reaction mixture viscosity, so the rate of reaction is increased by the improved mass transfer [41]. However, excess of methanol can lead to the emulsification of glycerol, which can recombine with the esters to reduce the biodiesel yield. In addition, excess amount of methanol can deactivate the lipase by changing its globular structure [42,43]. In the current study, a 6:1 methanol to oil ratio was observed to be the optimum CH_3OH concentration for the biocatalytic transesterification of waste cooking oil.

Water presence influences the activity of the immobilized enzyme and stability of the free enzyme. Water/oil interface may also be required for better catalytic activity of lipase. Furthermore, the enzyme deactivation due to small chain alcohols can be prevented if the lipase is dispersed in water [43]. However, in the presence of higher content of water hydrolysis may compete with the methanolysis [44]. Therefore, water content is required to be adjusted with minimal content as per experimental requirements. Highest triglyceride conversion into biodiesel was obtained while using 0.6% H_2O content in present research. Temperature significantly effects the enzymatic transesterification. The activity of lipase increases with temperature till the optimum point, i.e., 37 °C, and a further increase in temperature can lead to denaturisation of lipase.

Similar conditions have also been investigated by other researchers. Ying and Dong obtained the maximum biodiesel yield using immobilized lipase with 31.3% nano-biocatalyst, 38 °C temperature and 4.7:1 methanol to oil ratio [27]. Thangaraj et al. reported the maximum biodiesel yield of 89% at an optimum condition i.e., 1:3 methanol/oil ratio, 12 h of reaction period and 45 °C temp., using the immobilized NS81006 lipase as the catalyst [45]. Iso et al. reported the highest enzyme activity at 0.3% water content using immobilized lipase [46]. Mumtaz et al., using enzymatic transesterification, reported 95.9% biodiesel yield with 0.75% NOVOZYME-435, 6:1 methanol to oil ratio and 60 h of reaction at 32.50 °C [47]. Arumugam and Ponnusami used lipase immobilized on activated carbon for biodiesel production; optimum parameters were 1:9 oil to methanol ratio, 10% water content and 30 °C temperature, achieving a yield of 94.5% biodiesel with these conditions [41]. Xia also used RSM to optimize the enzymatic transesterification process, the optimum conditions reported are 4:1 methanol to oil ratio, 6.8% of biocatalyst and 42.2 °C reaction temperature [26]. Andrade et al. used nano-biocatalyst prepared by immobilization of lipase on magnetic nano-particles and achieved the highest biodiesel yield at 4:1 methanol/oil raio, 20% enzyme conc., 37 °C temp., and 12 h of time period [25]. Andrade et al. attained 95.5% methyl ester yield at 8:1 molar ratio of alcohol to oil, 8% biocatalyst amount and 45 °C temperature [48].

Table 1. Optimum reaction conditions for biodiesel production from Fe_3O_4-PDA-Liapase catalysed transesterification.

Feedstock	Catalyst	Catalyst Conc. (%)	Methanol to Oil Ratio (%)	Reaction Time (h)	Reaction Temp. (°C)	Water Conc. (%)	Biodiesel Yield (%)
WCO	Fe_3O_4_PDA_Lipase	10	6:1	30	37	0.6	92

3.2.5. Model Validation

Triplicate reactions were executed at optimum conditions to validate model accuracy. The average yield of 92.0 ± 1.3% was revealed to be comparable with that of predicted value, which was 88.93%. Hence, the model was depicted to be accurate and valid to estimate the response, i.e., yield of biodiesel.

3.2.6. ANOVA for Response Surface Quadratic Models for Biodiesel Production

For biodiesel production catalysed by Fe_3O_4_PDA_Lipase, quadratic model was depicted to be most suitable one with p-value < 0.05. The adjusted R^2 value for quadratic model was found to be 0.9840, while the lack of fit value was 0.0531. Insignificant lack of fit test value in addition to R^2 values also suggested/ascertained the fitness of quadratic model for Fe_3O_4_PDA_Lipase catalysed transesterification reactions.

Table 2 presents ANOVA describing selected model significance along with the significance of understudy reaction conditions. Out of the linear terms; A—methanol to oil ratio, B—enzyme concentration, C—reaction temperature and D—reaction time were ascertained to be significant, having p-values less than 0.05. While p-value i.e., 0.0874 > 0.05 depicted non-significant impact of E—water concentration. The above said factors significantly affected to the response as linear interactions i.e., AB, AC, AD, BD, and BE with p-values of 0.0010, 0.0321, 0.0076, 0.0008 and 0.0201 < 0.05, respectively. A^2, B^2 and C^2 were found to have significant effect with p-values 0.0245, < 0.0001 and < 0.0001, whilst D^2 and E^2 were insignificant quadratic term.

Model equation in terms of coded values is as follow;

$$\text{Biodiesel yield} = +86.03 + 1.97\,A + 14.73\,B + 0.97\,C + 2.24\,D - 0.68\,E + 1.45\,AB - 0.89$$
$$AC - 1.13\,AD + 0.76\,AE + 0.51\,BC + 1.47\,BD - 0.97\,BE - 0.57\,CD + 0.22\,CE + 0.053$$
$$DE - 3.37\,A^2 - 11.87\,B^2 - 8.90\,C^2 - 1.57\,D^2 - 1.72\,E^2$$

By the comparison of the factor's coefficients in the equation, the relative impact of each factor on the biodiesel yield can be identified.

Table 2. ANOVA for response surface quadratic model for biodiesel yield.

Source	Df	Sum of Squares	Mean Square	F Value	p-Value Prob > F
Model	20	15,145.61	757.28	151.53	<0.0001
A—methanol to oil ratio	1	132.56	132.56	26.53	<0.0001
B—enzyme concentration	1	7374.92	7374.92	1475.73	<0.0001
C—reaction temperature	1	32.22	32.22	6.45	0.0167
D—reaction time	1	170.11	170.11	34.04	<0.0001
E—water	1	15.64	15.64	3.13	0.0874
AB	1	67.57	67.57	13.52	0.0010
AC	1	25.34	25.34	5.07	0.0321
AD	1	41.18	41.18	8.24	0.0076
AE	1	18.45	18.45	3.69	0.0645
BC	1	8.44	8.44	1.69	0.2041
BD	1	69.33	69.33	13.87	0.0008
BE	1	30.23	30.23	6.05	0.0201
CD	1	10.59	10.59	2.12	0.1563
CE	1	1.61	1.61	0.32	0.5744
DE	1	0.090	0.090	0.018	0.8940
A^2	1	28.12	28.12	5.63	0.0245
B^2	1	348.60	348.60	69.76	<0.0001
C^2	1	188.78	188.78	37.78	<0.0001
D^2	1	6.11	6.11	1.22	0.2779
E^2	1	7.33	7.33	1.47	0.2355
Residual	29	144.93	5.00		
Lack of Fit	22	132.35	6.02	3.35	0.0531
Pure Error	7	12.58	1.80		
Cor Total	49	15,290.53			

Li and Yan [49] applied three factor RSM for the optimization of transesterification process using immobilized lipase as catalyst, enzyme conc. and temp. were ascertained to be significant linear terms, but methanol to oil ratio was insignificant term with (*p*-value of 0.3083) all quadratic terms were also significant, while no first order interaction term was significant (Table 2). Wu et al. [50] optimized four reaction parameters using RSM, which were (i) lipase concentration, (ii) reaction time, (iii) reaction temperature, and (iv) ethanol to oil molar ratio. Lipase level, temperature and time were revealed to be the significant linear terms that support the present study, while ethanol to oil ratio showed insignificant impact, which might be due to the shorter range (3:1 to 6:1) of alcohol: oil used in that design. (Time × Temperature) was the only significant first order interaction terms. Huang et al. [51] reported a significant quadratic model for the optimization of methyl ester formation. Lipase to oil ratio (x_1), ratio of two lipases (x_2), t-butanol:oil (x_3), methanol:oil (x_4) and time (x_5) were independent variables chosen for optimization of reaction. Out of that, all the linear terms showed significant effect, while x_1x_2, x_2x_3, x_3x_4, x_2x_4, x_1x_4, and x_4x_5 were significant first order terms and among quadratic terms x_3^2 and x_4^2 had significant effect on response. Li and Dong [27] selected methanol:oil x_1, lipase:oil x_2, water content x_3, and temperature x_4 as independent variables for process optimization of biodiesel production using RSM. All the linear terms were significant in that model as well, which resembles the current study except the water content, which is insignificant in our work. All quadratic and first order interaction terms were also significant, expect for x_1x_4 and x_2x_4, and similar first order terms are insignificant in the present work as well. Xia [26] reported methanol:oil, amount of enzyme, time for reaction and amount of hexane (solvent) as significant linear terms, all the quadratic terms showed significant impact/effect on response, while (enzyme × hexane content) was the only significant first order interaction term. The results of ANOVA for the optimization of biodiesel production using immobilized lipase are comparable to the literature; the few variations might be due to different fatty acid profiles, different ranges of selected parameters, different alcohols being used and because of using solvent/solvent free systems.

Predicted vs. actual plot (Figure 8) of % biodiesel yield for the design, depict the fitness of the quadratic model, the difference between the predicted and the actual values are very small, as presented in Figure 8, which confirms the fitness of quadratic model. Our findings are comparable to the previous reports [27,51].
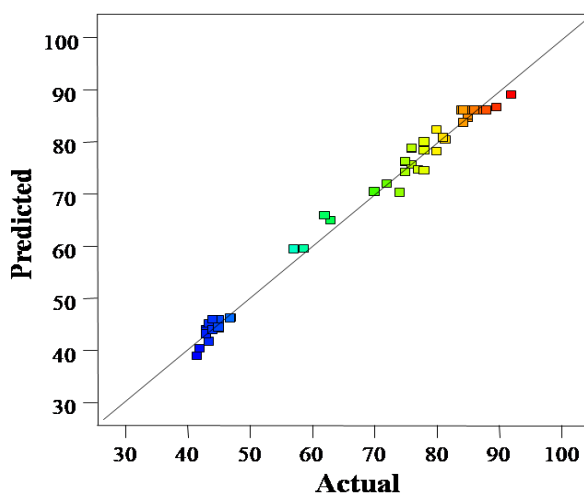

Figure 8. Predicted vs. actual values plot.

3.2.7. Response Surface (RS) Plots of Interacting Terms

RS plots of the significant first order interaction terms are presented in Figure 9. Figure 9a is the RS plot for biocatalyst (Fe$_3$O$_4$_PDA_Lipase) concentration and methanol to oil ratio. 3D plot revealed that the biodiesel yield increases with the increase in biocatalyst concentration and the content of methanol

as the highest biodiesel yield is obtained at a biocatalyst concentration of 10% and 6:1 methanol to oil ratio, with further increase in the methanol content the yield starts to decrease, which might be due to deactivation of the enzyme by excess methanol. Figure 9b indicates the effect of methanol to oil ratio and reaction temperature interaction. The highest response value at the centre shows that the yield increases with temperature and methanol to oil ratio till the optimum points, then increase in temperature and methanol content results in decreased in biodiesel yield. Figure 9c 3D plot describes the influence of reaction time and methanol: oil ratio on response. Figure 9d is the response surface plot of enzyme concentration (%) and reaction time (h). The highest response at the inner corner presents that the biodiesel yield increases with both reaction time and the biocatalyst concentration, as the highest yield is obtained at 10% biocatalyst concentration and 30 h of reaction time. BE (enzyme conc. × water content) is another significant interaction term. The enzyme activity and structure are affected by the water content, which is clearly indicated by Figure 9e, which predicts that the biodiesel yield decreases by reduced enzyme activity as the water percentage deviates from optimum value.
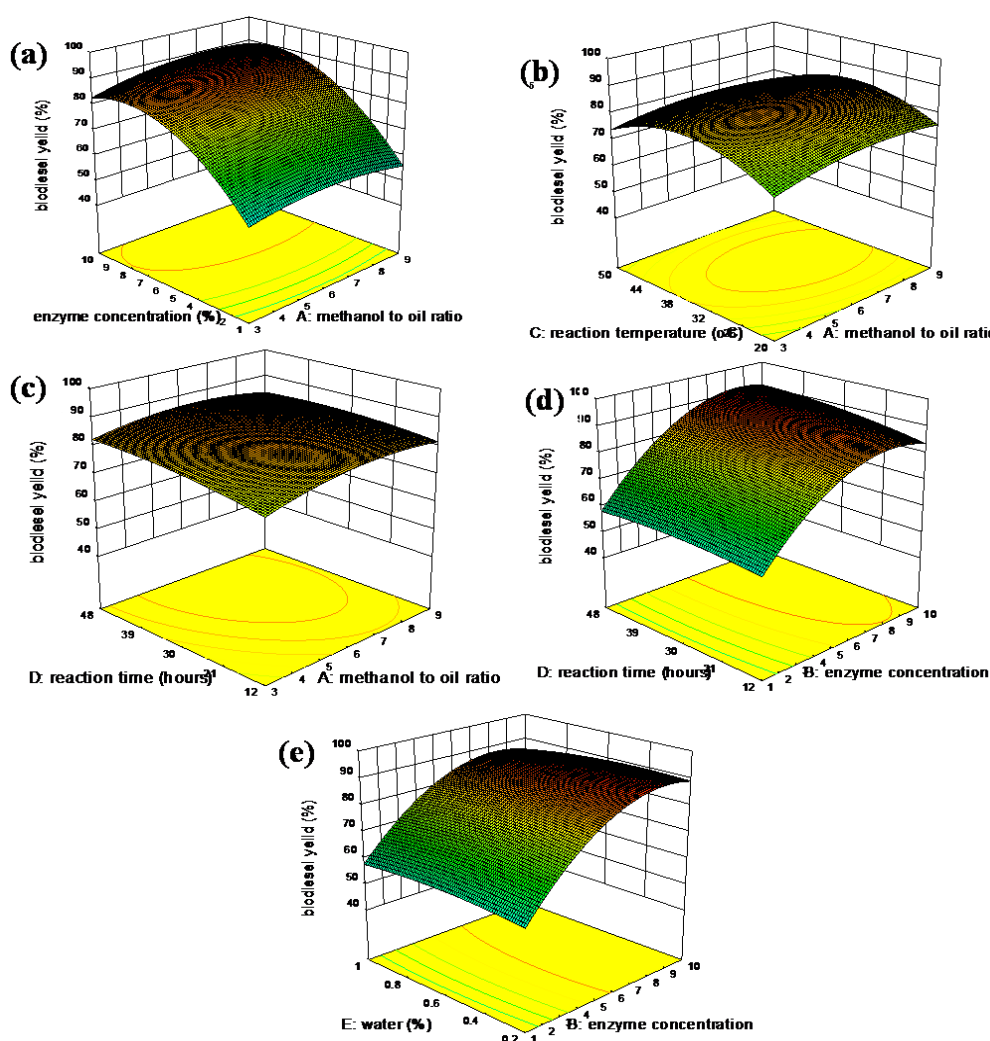

Figure 9. Response surface graphs of significant first order interaction terms (**a**) A × B, (**b**) A × C, (**c**) A × D, (**d**) B × D and (**e**) B × E.

3.2.8. Recovery and Reusability of Nano-Biocatalyst

At reaction completion, Fe_3O_4_PDA_Lipase was recovered by using magnetic decantation. Afterwards, lipase assay was carried out to find out the activity of immobilized lipase after recovery. No change in the activity of lipase was detected after first use, i.e., 17.83 U/mg/min. Therefore,

these recovered Fe_3O_4 magnetic nanoparticles were reused several times for the biodiesel production and after the completion of each reaction the lipase activity assay was performed, which showed that lipase activity started decreasing after four uses, and after seven uses the activity declined to 4.6 U/mg/min. The biodiesel conversion rate decreased after four uses (Figure 10), which was clearly due to a decrease in the activity of immobilized lipase. This reduction in activity may be due to the exposure of nano-biocatalyst to organic solvents present in the reaction mixture or repeated exposure to heat, which may have resulted in the decrease of lipase activity. Similar studies have also been reported by Dumri and Hung [23].
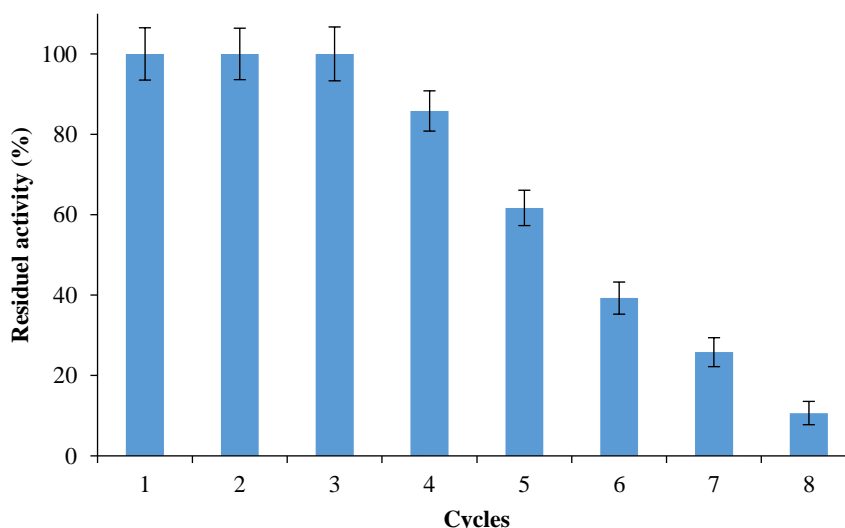

Figure 10. Re-usability of lipase immobilized Fe_3O_4 nanoparticles.

3.2.9. Physical Properties of Biodiesel

Fuel properties of produced biodiesel are presented in Table 3. The fuel properties meet the biodiesel standards set by ASTMD.

Table 3. Properties of WCO based biodiesel.

Property	Unit	Value	ASTM D	Method
Acid value	(mg KOH/g)	0.21 ± 0.06	<0.50	ASTM D 664
Kinematic viscosity (40 °C)	(mm^2/s)	4.10 ± 0.04	1.9–6.0	ASTM D 445
Flash point	(°C)	170.41 ± 0.47	>130	ASTM D 93
Pour point	(°C)	−3.0 ± 0.5	-	ASTM D 97
Density	(g mL^{-1})	0.871 ± 0.320	0.86–0.90	ASTM D 5002

For the complete combustion of biodiesel, optimum fuel to air ratio is required, which is obtained at specific levels of density. Kinematic viscosity is a measure of restriction between the two layers of a liquid, and quality of combustion is recognized to be affected by kinematic viscosity. The ignition point of fuel on exposure to the spark is called the flash point. High flash points of the biodiesel make it easy to store. Pour point and cloud point are important for cold flow properties. Furthermore, suitability of biodiesel for the use in engine can also be evaluated by these properties. Previous studies have revealed comparable results for the biodiesel produced from WCO. Few variations in the observed fuel characteristics may be attributed to different source and composition of feedstock oil [33].

4. Conclusions

Fe_3O_4_PDA_Lipase nano-biocatalyst was successfully synthesized and utilized to produce biodiesel using waste cooking oil as feedstock. Using a best fitted quadratic model, different reaction

conditions of biodiesel production process were optimized, and it was revealed that Fe₃O₄_PDA_Lipase actively catalysed the reaction, resulting in a highlight biodiesel yield i.e., 92%. The synthesized nano-biocatalyst proved to have better adoptability/stability and was easily recoverable using external magnet and retained most of its catalytic activity for four cycles. The properties of synthesized biodiesel were in agreement with the ASTM D standards. Conclusively, Fe₃O₄_PDA_Lipase has been proved to be a sustainable and cost-effective catalyst for biodiesel production.

Author Contributions: The conceptualization of this journal article is from T.T., M.W.M. and U.R.; the methodology was designed by T.T., M.W.M. and U.R.; the writing—original draft was prepared by T.T.; S.A., A.S. and M.W.M. helped with the editing and supervision. H.M. provided technical assistance regarding the synthesis and characterization of nano-biocatalyst, A.I., T.S.Y.C. and I.A.N. reviewed the manuscript for final version improvement. All authors have read and agreed to the published version of the manuscript.

Conflicts of Interest: The authors declare no conflict of interest.

References

1. Shirneshan, A. HC, CO, CO₂ and NOₓ emission evaluation of a diesel engine fueled with waste frying oil methyl ester. *Procedia-Soc. Behav. Sci.* **2013**, *75*, 292–297. [CrossRef]

2. Srivastava, A.; Prasad, R. Triglycerides-based diesel fuels. *Renew. Sustain. Energy Rev.* **2000**, *4*, 111–133. [CrossRef]

3. Mehrasbi, M.R.; Mohammadi, J.; Peyda, M.; Mohammadi, M. Covalent immobilization of Candida antarctica lipase on core-shell magnetic nanoparticles for production of biodiesel from waste cooking oil. *Renew. Energy* **2017**, *101*, 593–602. [CrossRef]

4. Gui, M.M.; Lee, K.T.; Bhatia, S. Feasibility of edible oil vs. non-edible oil vs. waste edible oil as biodiesel feedstock. *Energy* **2008**, *33*, 1646–1653. [CrossRef]

5. Aladedunye, F.A.; Przybylski, R. Degradation and Nutritional Quality Changes of Oil During Frying. *J. Am. Oil Chem. Soc.* **2008**, *86*, 149–156. [CrossRef]

6. Paul, S.; Mittal, G.S. Regulating the use of degraded oil/fat in deep-fat/oil food frying. *Crit. Rev. Food Sci. Nutr.* **1997**, *37*, 635–662. [CrossRef]

7. Raqeeb, M.A.; Bhargavi, R. Biodiesel production from waste cooking oil. *J. Chem. Pharm. Res.* **2015**, *7*, 670–681.

8. Zhang, H.; Ding, J.; Zhao, Z. Microwave assisted esterification of acidified oil from waste cooking oil by CERP/PES catalytic membrane for biodiesel production. *Bioresour. Technol.* **2012**, *123*, 72–77. [CrossRef]

9. Balat, M.; Balat, H. Progress in biodiesel processing. *Appl. Energy* **2010**, *87*, 1815–1835. [CrossRef]

10. Karmakar, A.; Karmakar, S.; Mukherjee, S. Properties of various plants and animals' feedstocks for biodiesel production. *Bioresour. Technol.* **2010**, *101*, 7201–7210. [CrossRef]

11. Fukuda, H.; Kondo, A.; Noda, H. Biodiesel fuel production by transesterification of oils. *J. Biosci. Bioeng.* **2001**, *92*, 405–416. [CrossRef]

12. Köse, Ö.; Tüter, M.; Aksoy, H.A. Immobilized Candida antarctica lipase-catalyzed alcoholysis of cotton seed oil in a solvent-free medium. *Bioresour. Technol.* **2002**, *83*, 125–129. [CrossRef]

13. Bisen, P.S.; Sanodiya, B.S.; Thakur, G.S.; Baghel, R.K.; Prasad, G. Biodiesel production with special emphasis on lipase-catalyzed transesterification. *Biotechnol. Lett.* **2010**, *32*, 1019–1030. [CrossRef] [PubMed]

14. Sheldon, R.A.; Van Pelt, S. Enzyme immobilisation in biocatalysis: Why, what and how. *Chem. Soc. Rev.* **2013**, *42*, 6223–6235. [CrossRef] [PubMed]

15. Al-Zuhair, S.; Dowaidar, A.; Kamal, H. Dynamic modeling of biodiesel production from simulated waste cooking oil using immobilized lipase. *Biochem. Eng. J.* **2009**, *44*, 256–262. [CrossRef]

16. Rossi, L.M.; Costa, N.J.S.; Silva, F.P.; Gonçalves, R.V. Magnetic nanocatalysts: Supported metal nanoparticles for catalytic applications. *Nanotechnol. Rev.* **2013**, *2*, 5. [CrossRef]

17. Matsunaga, T.; Kamiya, S. Use of magnetic particles isolated from magnetotactic bacteria for enzyme immobilization. *Appl. Microbiol. Biotechnol.* **1987**, *26*, 328–332. [CrossRef]

18. Wang, C.; Han, H.; Jiang, W.; Ding, X.; Li, Q.; Wang, Y. Immobilization of thermostable lipase QLM on core-shell structured polydopamine-coated Fe₃O₄ nanoparticles. *Catalysts* **2017**, *7*, 49. [CrossRef]

19. Adlercreutz, P. Immobilisation and application of lipases in organic media. *Chem. Soc. Rev.* **2013**, *42*, 6406–6436. [CrossRef]

20. Lee, H.; Rho, J.; Messersmith, P.B. Facile Conjugation of Biomolecules onto Surfaces via Mussel Adhesive Protein Inspired Coatings. *Adv. Mater.* **2009**, *21*, 431–434. [CrossRef]

21. Ren, Y.; Rivera, J.G.; He, L.; Kulkarni, H.; Lee, D.K.; Messersmith, P.B. Facile, high efficiency immobilization of lipase enzyme on magnetic iron oxide nanoparticles via a biomimetic coating. *BMC Biotechnol.* **2011**, *11*, 63. [CrossRef] [PubMed]

22. Guo, S.; Li, D.; Zhang, L.; Li, J.; Wang, E. Monodisperse mesoporous superparamagnetic single-crystal magnetite nanoparticles for drug delivery. *Biomaterials* **2009**, *30*, 1881–1889. [CrossRef] [PubMed]

23. Dumri, K.; Hung Anh, D. Immobilization of Lipase on Silver Nanoparticles via Adhesive Polydopamine for Biodiesel Production. *Enzyme Res.* **2014**, *2014*, 389739. [CrossRef] [PubMed]

24. Shabbir, A.; Mukhtar, H. Optimization process for enhanced extracellular lipases production from a new isolate of Aspergillus terreus ah-F2. *Pak. J. Bot.* **2018**, *50*, 1571–1578.

25. Andrade, M.F.C.; Parussulo, A.L.A.; Netto, C.G.C.M.; Andrade, L.H.; Toma, H.E. Lipase immobilized on polydopamine-coated magnetite nanoparticles for biodiesel production from soybean oil. *Biofuel Res. J.* **2016**, *3*, 403–409. [CrossRef]

26. Li, Y.X. Optimization of biodiesel production from rice bran oil via immobilized lipase catalysis. *Afr. J. Biotechnol.* **2011**, *10*, 16314–16324.

27. Li, Y.X.; Dong, B.X. Optimization of Lipase-Catalyzed Transesterification of Cotton Seed Oil for Biodiesel Production Using Response Surface Methodology. *Braz. Arch. Biol. Technol.* **2016**, *59*. [CrossRef]

28. Soltani, S.; Rashid, U.; Yunus, R.; Taufiq-Yap, Y.H.; Al-Resayes, S.I. Post-functionalization of polymeric mesoporous C@Zn core-shell spheres used for methyl ester production. *Renew. Energy* **2016**, *99*, 1235–1243. [CrossRef]

29. Cao, X.; Zhang, B.; Zhao, F.; Feng, L. Synthesis and properties of MPEG-coated superparamagnetic magnetite nanoparticles. *J. Nanomater.* **2012**, *2012*, 607296. [CrossRef]

30. Chen, D.; Tang, Q.; Li, X.; Zhou, X.; Zang, J.; Xue, W.-Q.; Xiang, J.-Y.; Guo, C.-Q. Biocompatibility of magnetic Fe_3O_4 nanoparticles and their cytotoxic effect on MCF-7 cells. *Int. J. Nanomed.* **2012**, *7*, 4973. [CrossRef]

31. Baharfar, R.; Mohajer, S. Synthesis and Characterization of Immobilized Lipase on Fe_3O_4 Nanoparticles as Nano biocatalyst for the Synthesis of Benzothiazepine and Spirobenzothiazine Chroman Derivatives. *Catal. Lett.* **2016**, *146*, 1729–1742. [CrossRef]

32. Noshadi, I.; Amin, N.A.S.; Parnas, R.S. Continuous production of biodiesel from waste cooking oil in a reactive distillation column catalyzed by solid heteropolyacid: Optimization using response surface methodology (RSM). *Fuel* **2012**, *94*, 156–164. [CrossRef]

33. Uzun, B.B.; Kılıç, M.; Özbay, N.; Pütün, A.E.; Pütün, E. Biodiesel production from waste frying oils: Optimization of reaction parameters and determination of fuel properties. *Energy* **2012**, *44*, 347–351. [CrossRef]

34. Kannan, G.; Anand, R. Effect of injection pressure and injection timing on DI diesel engine fuelled with biodiesel from waste cooking oil. *Biomass Bioenergy* **2012**, *46*, 343–352. [CrossRef]

35. Omar, W.N.N.W.; Amin, N.A.S. Optimization of heterogeneous biodiesel production from waste cooking palm oil via response surface methodology. *Biomass Bioenergy* **2011**, *35*, 1329–1338. [CrossRef]

36. Patil, P.D.; Gude, V.G.; Reddy, H.K.; Muppaneni, T.; Deng, S. Biodiesel production from waste cooking oil using sulfuric acid and microwave irradiation processes. *J. Environ. Protect.* **2012**, *3*, 107. [CrossRef]

37. Dubé, M.A.; Zheng, S.; McLean, D.D.; Kates, M. A comparison of attenuated total reflectance-FTIR spectroscopy and GPC for monitoring biodiesel production. *J. Am. Oil Chem. Soc.* **2004**, *81*, 599–603. [CrossRef]

38. Siatis, N.; Kimbaris, A.; Pappas, C.; Tarantilis, P.; Polissiou, M. Improvement of biodiesel production based on the application of ultrasound: Monitoring of the procedure by FTIR spectroscopy. *J. Am. Oil Chem. Soc.* **2006**, *83*, 53–57. [CrossRef]

39. Soares, I.P.; Rezende, T.F.; Silva, R.C.; Castro, E.V.R.; Fortes, I.C. Multivariate calibration by variable selection for blends of raw soybean oil/biodiesel from different sources using Fourier transform infrared spectroscopy (FTIR) spectra data. *Energy Fuel* **2008**, *22*, 2079–2083. [CrossRef]

40. Stergiou, P.Y.; Foukis, A.; Filippou, M.; Koukouritaki, M.; Parapouli, M.; Theodorou, L.G.; Hatziloukas, E.; Afendra, A.; Pandey, A.; Papamichael, E.M. Advances in lipase-catalyzed esterification reactions. *Biotechnol. Adv.* **2013**, *31*, 1846–1859. [CrossRef]

41. Arumugam, A.; Ponnusami, V. Production of biodiesel by enzymatic transesterification of waste sardine oil and evaluation of its engine performance. *Heliyon* **2017**, *3*, e00486. [CrossRef] [PubMed]

42. Christopher, L.P.; Kumar, H.; Zambare, V.P. Enzymatic biodiesel: Challenges and opportunities. *Appl. Energy* **2014**, *119*, 497–520. [CrossRef]

43. Kulschewski, T.; Sasso, F.; Secundo, F.; Lotti, M.; Pleiss, J. Molecular mechanism of deactivation of *C. antarctica* lipase B by methanol. *J. Biotechnol.* **2013**, *168*, 462–469. [CrossRef] [PubMed]

44. Zhao, X.; Qi, F.; Yuan, C.; Du, W.; Liu, D. Lipase-catalyzed process for biodiesel production: Enzyme immobilization, process simulation and optimization. *Renew. Sustain. Energy Rev.* **2015**, *44*, 182–197. [CrossRef]

45. Thangaraj, B.; Jia, Z.; Dai, L.; Liu, D.; Du, W. Lipase NS81006 immobilized on Fe_3O_4 magnetic nanoparticles for biodiesel production. *Ovidius Univ. Ann. Chem.* **2016**, *27*, 13–21. [CrossRef]

46. Iso, M.; Chen, B.; Eguchi, M.; Kudo, T.; Shrestha, S. Production of biodiesel fuel from triglycerides and alcohol using immobilized lipase. *J. Mol. Catal. B Enzymat.* **2001**, *16*, 53–58. [CrossRef]

47. Mumtaz, M.W.; Adnan, A.; Mahmood, Z.; Mukhtar, H.; Malik, M.F.; Qureshi, F.A.; Raza, A. Biodiesel from Waste Cooking Oil: Optimization of Production and Monitoring of Exhaust Emission Levels From its Combustion in a Diesel Engine. *Int. J. Green Energy* **2012**, *9*, 685–701. [CrossRef]

48. Andrade, I.C.; Vargas, F.E.S.; Fajardo, C.A.G. Biodiesel production from waste cooking oil by enzymatic catalysis process. *J. Chem. Eng.* **2013**, *7*, 993–1000.

49. Li, Q.; Yan, Y. Production of biodiesel catalyzed by immobilized Pseudomonas cepacia lipase from Sapiumsebiferum oil in micro-aqueous phase. *Appl. Energy* **2010**, *87*, 3148–3154. [CrossRef]

50. Wu, W.; Foglia, T.; Marmer, W.; Phillips, J. Optimizing production of ethyl esters of grease using 95% ethanol by response surface methodology. *J. Am. Oil Chem. Soc.* **1999**, *76*, 517–521. [CrossRef]

51. Huang, Y.; Zheng, H.; Yan, Y. Optimization of lipase-catalyzed transesterification of lard for biodiesel production using response surface methodology. *Appl. Biochem. Biotechnol.* **2010**, *160*, 504–515. [CrossRef] [PubMed]